

Estimating the dark matter halo velocity and surface temperature of some known pulsars due to dark matter capture

Debashree Sen^a Atanu Guha,^{b,1}

^aCenter for Extreme Nuclear Matters (CENuM), Korea University, Seoul 02841, Korea

^bDepartment of Physics, Chungnam National University, 99, Daehak-ro, Yuseong-gu, Daejeon-34134, South Korea

E-mail: debashreesen88@gmail.com, atanu@cnu.ac.kr

Abstract. Considering four known pulsars J1906+0746, J1933-6211, J2043+1711 and the Vela pulsar, we study the scenario of dark matter (DM) capture in neutron stars (NSs). For the purpose we choose four well-known relativistic mean field models to obtain the radius corresponding to the observed mass of these pulsars and consequently the scattering cross-section of DM with the different particles of the β stable NS matter. The estimated DM-electron scattering cross-section in this work is stringent compared to the current direct detection experimental probe. We then compute the lower limit on the halo velocity of DM for the four pulsars from the knowledge of the upper limit on effective temperature of the individual pulsars. We also extend our work to calculate the value of the effective temperature with the different models using the fitted values of the halo velocity of DM of the four pulsars with respect to their distances from the galactic center. Our findings are consistent with the analysis of the observed data.

¹Corresponding author

Contents

1	Introduction	1
2	Formalism	2
2.1	Models	2
2.2	Dark matter capture and threshold scattering cross-section	3
2.3	Lower limit on v_{halo}	3
2.4	Effective temperature from v_{halo} data	4
3	Results and Discussions	5
3.1	Dark matter capture and lower limit on v_{halo}	5
3.2	Effective temperature from v_{halo} data	5
3.3	Dark matter scattering cross-section	6
4	Summary and Conclusion	7
A	Distance of pulsars from galactic center	8

1 Introduction

The lion's share of the total energy budget of the Universe is made up of dark energy (about 70%) while the succeeding leading component is dark matter (around 25%). Only 5% of the energy content consists of so-called luminous matter or the baryonic matter. This is nowadays an unambiguously evident fact supported by a numerous astrophysical and cosmological observations [1–4]. Over the last few decades several dedicated search methods have been implemented to get an idea about the interaction strength between the dark matter (DM) and standard model (SM) particles. Among the popular experimental search avenues, significant developments have been made for the direct and indirection detection strategies [5, 6]. The most stringent constraints are obtained till date by the leading direct detection experiments like SuperCDMS [7], XENONnT [8], PandaX-II [9], DarkSide-50 [10], SENSEI [11] and LUX-ZEPLIN [12]. Experiments dedicated to indirect search are FERMI-LAT [13], IceCube [14], PAMELA [15, 16], AMS-02 [17], Voyager [18] and CALET [19, 20].

Alongside the progress of the experimental probes, there are significant advancement in the phenomenological aspects as well. One of the well motivated methods to understand the properties of the DM particles is to explore the DM capture by neutron stars (NSs) as suggested by the recent literature [21–25]. NSs are the most dense objects present in our Universe which are accessible by direct observations. They serve the purpose of being a unique natural astrophysical laboratory where we can investigate the properties of matter under extreme conditions. Apart from DM capture by NSs, there are several other mechanisms which can be responsible for the possible presence of DM in NSs, e.g., creation of its own DM through dark decays of neutrons [26–29] or inheritance of DM from the supernovae [30] etc. For the present work we are interested in the accretion mechanism. Due to strong gravitational pull, halo DM particles fall into NS and become a structural part of it [31–37]. Through this accretion process DM gets captured by NS which allows us to explore the interaction strength between DM and SM particles.

The accreted DM particles lose kinetic energy due to collisions with the matter inside the NS and dump the energy to the NS which in turn heat up the NS. This phenomena can manifest itself as the non-zero surface temperature (T_S) of sufficiently cold NSs and the mechanism of kinetic heating can be an observable signature of DM. Due to the self interactions, the DM particles attain thermal equilibrium among themselves and become gravitationally bound to the NS [23, 38]. Recent successful observations by the Chandra and XMM-Newton [39] are reliable and provide an upper bound on the effective temperature (T_∞) of the NS surface as seen by a distant observer [40, 41].

We organize the present work as follows. In the next Sec. 2, we briefly address the framework of the four Relativistic Mean Field (RMF) hadronic models, viz., TM1 [42], GM1 [43], DD2 [44] and DD-MEX [45]. In the same section, we also discuss the mechanism of estimating the threshold values for the DM-SM scattering cross-section (σ_{th}^i) with different constituents of the β stable NS matter. Additionally, we formulate the lower limit on the DM halo velocity (v_{halo}^l) from the knowledge of the upper bound on T_∞ [40, 41] and on the other hand we present an analytical form for the T_∞ from the known v_{halo} data [46]. We then present the results of our estimations based on Sec. 2 and corresponding discussions in Sec. 3 for some known pulsars like J1906+0746, J1933-6211, J2043+1711 and the Vela pulsar, whose mass, position and distance with respect to earth are observationally known. In the absence of any concrete observational data for the radius of these four pulsars, the four RMF models are used to determine the radius of these pulsars corresponding to their masses in order to calculate σ_{th}^i . We summarize and conclude in the final section 4 of the paper.

2 Formalism

2.1 Models

We consider four well-known RMF models. Of them, TM1 [42] and GM1 [43] are with non-linear self couplings while DD2 [44] and DD-MEX [45] have density-dependent couplings following the Typel-Wolter ansatz [47]. The values of the couplings and the saturation properties (like the saturation density ρ_0 , the symmetry energy J_0 , the slope parameter L_0 , nuclear incompressibility K_0 , skewness coefficient S_0 , and the curvature parameter K_{sym} of the nuclear symmetry energy) of all the above four models considered in this present work, can be found in the respective references and also in [48]. Also the detailed methodology for obtaining the equation of state (EoS) of β equilibrated NS matter using these four models can be found in the respective references and in [33, 48].

For the obtained EoS, we compute the radius (R_{NS}) corresponding to the observed mass (M_{NS}) of the pulsars J1906+0746, J1933-6211, J2043+1711 and the Vela pulsar, with the help of the Tolman-Oppenheimer-Volkoff (TOV) equations [49, 50]. M_{NS} of J1906+0746, J1933-6211, and J2043+1711 is taken from https://www3.mpifr-bonn.mpg.de/staff/pfreire/NS_masses.html while that of the Vela pulsar from [51]. In Tab. 1 we specify the measured quantities like the observed mass (M_{NS}), distance from the earth (d), right ascension (RA) and declination (Dec) of these four pulsars used to obtain the results of our present work.

Table 1: Some known pulsars and measured quantities like mass (M_{NS}), distance from the earth (d), right ascension (RA) and declination (Dec). M_{NS} of J1906+0746, J1933-6211, and J2043+1711 is taken from https://www3.mpifr-bonn.mpg.de/staff/pfreire/NS_masses.html and that of the Vela pulsar from [51]

Pulsar	M_{NS} (M_{\odot})	d (kpc)	RA	Dec
J1906+0746	1.29(11)	7.4	19h 06m 48.86s	07° 46' 25.9"
J1933-6211	1.4^{+3}_{-2}	0.65	19h 33m 32.43s	-62° 11' 46.88"
J2043+1711	1.38^{+12}_{-13}	1.389	20h 43m 20.88s	17° 11' 28.89"
Vela	1.88 ± 0.13	0.28	08h 35m 20.61s	-45° 10' 34.87"

2.2 Dark matter capture and threshold scattering cross-section

The threshold scattering cross-section (σ_{th}^i) of the DM with the i -th particle can be obtained following [23] as

$$\sigma_{th}^i = \frac{\pi R_{NS}^2 k_i}{N_i q}, \quad \text{if } q < k_i$$

$$\text{otherwise } k_i/q = 1 \quad (2.1)$$

where, k_i is the Fermi momentum of the i -th species. Since we consider β equilibrated NS matter, $i = n, p, e, \mu$ and N_i is the total individual particle density up to R_{NS} , obtained by radially integrating the density profile $N_i(r)$ of each particle obtained at different values of the radius up to R_{NS} . The momentum transfer q is given as

$$q = (\gamma_{esc} - 1)m_{\chi}v_{\chi} \quad (2.2)$$

where, m_{χ} is the mass of the captured fermionic DM and v_{χ} its velocity. We have

$$v_{\chi} = v_{esc} = \frac{\sqrt{\gamma_{esc}^2 - 1}}{\gamma_{esc}} \quad (2.3)$$

because we have considered maximum impact for incident DM following [24] and

$$\gamma_{esc} = 1 + \frac{2M_{NS}}{R_{NS}} \quad (2.4)$$

2.3 Lower limit on v_{halo}

We follow [23, 24] to obtain the lower limit on v_{halo} i.e. the velocity of DM at NS halo before capture. The surface temperature T_S of NS can be obtained in terms of the upper limit on effective temperature T_{∞} [52] as

$$T_S = \frac{T_{\infty}}{\sqrt{1 - \frac{2M_{NS}}{R_{NS}}}} \quad (2.5)$$

Adopting the upper limit of T_{∞} for the four pulsars considered from [40, 41], we obtain the upper limit on T_S and consequently on the energy deposited per unit time by DM (\dot{k}) using the expression

$$\dot{k} \left(1 - \frac{2M_{NS}}{R_{NS}} \right) = 4\pi R_{NS}^2 \sigma_{SB} T_S^4 \quad (2.6)$$

where, the Stefan-Boltzman constant $\sigma_{SB}=\pi^2/60$. The kinetic energy at the surface when the DM enters the NS is given as

$$E_S = (\gamma_{esc} - 1)m_\chi \quad (2.7)$$

Therefore we get

$$\dot{k} = E_S \frac{\dot{M}_\chi}{m_\chi} f \quad (2.8)$$

where, the DM mass passing through surface of NS per unit time (\dot{M}_χ) is given as

$$\dot{M}_\chi = \pi b_{max}^2 v_{esc} \rho_\chi \quad (2.9)$$

Here, the maximum impact parameter for the DM to intersect the NS surface is

$$b_{max} = R_{NS} \frac{v_{esc}}{v_{halo}} \gamma_{esc} \quad (2.10)$$

and ρ_χ is the mass density of DM halo. In Eq. 2.8, the capture fraction

$$f = \min \left[\frac{\sigma_\chi^i}{\sigma_{th}^i}, 1 \right] \quad (2.11)$$

Here, $f=1$ because we have considered the upper bound on T_∞ which always makes $f=1$. In [23] it is already mentioned that if $T_\infty > 1700$ Kelvin (NS blackbody temperature), the DM capture rate is maximum i.e., $f=1$.

Combining Eqs. 2.6 - 2.10 we have

$$\frac{\rho_\chi}{v_{halo}^2} = \frac{\dot{k}}{(\gamma_{esc} - 1) \pi R_{NS}^2 (\gamma_{esc}^2 - 1)^{3/2} \gamma_{esc}} \quad (2.12)$$

where, γ_{esc} is obtained from Eq. 2.4 in terms of M_{NS} and R_{NS} . As we have the upper limit on \dot{k} using the upper limit of T_∞ , we obtain lower limit on v_{halo} as v_{halo}^l from Eq. 2.12. Corresponding to the mass M_{NS} of each pulsar, we have four values of R_{NS} with four different RMF models TM1, GM1, DD2 and DD-MEX. Thus we have four slightly different upper limit of T_∞ for each pulsar. In Eq. 2.12 the ρ_χ for the four pulsars is obtained using the Navarro-Frenk-White (NFW) profile [53, 54] as

$$\rho_\chi(d_{GC}) = \frac{\rho_0}{\left(\frac{d_{GC}}{r_s}\right) \left(1 + \frac{d_{GC}}{r_s}\right)^2} \quad (2.13)$$

where, d_{GC} is the distance of the particular pulsar from galactic center, calculated in Appendix A using the values of the distance of pulsar from earth (d) and its RA and Dec. ρ_0 and r_s are the reference parameters [53, 54].

2.4 Effective temperature from v_{halo} data

We next calculate the surface temperature of the four individual pulsar considering the fitted values of v_{halo} data reported in [46] with respect to d_{GC} . Once we obtain the values of $\rho_\chi(d_{GC})$ for the individual pulsars and the values of v_{halo} from the fitted data corresponding to d_{GC} referring [46], we compute \dot{k} using Eq. 2.12 and consequently we obtain the values of surface temperature T_S from Eq. 2.6. Finally we compute the effective temperature T_∞ of each pulsar using Eq. 2.5. With four different RMF models, we have four slightly different values of T_∞ for each pulsar.

3 Results and Discussions

3.1 Dark matter capture and lower limit on v_{halo}

Table 2: Some known pulsars and their effective temperature (T_{∞}^{ul}) taken from [40, 41] and the obtained radius (R_{NS}), distance from galactic center (d_{GC}), and the lower limit on v_{halo} (v_{halo}^{ll}) with the four different RMF models.

Pulsar	d_{GC} (kpc)	$\log_{10} T_{\infty}$	Model	R_{NS} (km)	v_{halo}^{ll}
J1906+0746	5.55	5.93	TM1	12.47	3.495×10^{-9}
			GM1	12.23	3.534×10^{-9}
			DD2	11.99	3.572×10^{-9}
			DD-MEX	12.85	3.434×10^{-9}
J1933-6211	7.595	5.64	TM1	12.63	1.073×10^{-8}
			GM1	12.37	1.084×10^{-8}
			DD2	12.15	1.094×10^{-8}
			DD-MEX	12.98	1.058×10^{-8}
J2043+1711	7.572	5.91	TM1	12.60	3.085×10^{-9}
			GM1	12.35	3.116×10^{-9}
			DD2	12.13	3.143×10^{-9}
			DD-MEX	12.96	3.039×10^{-9}
Vela	8.14	5.82	TM1	12.93	4.833×10^{-9}
			GM1	12.65	4.841×10^{-9}
			DD2	12.52	4.844×10^{-9}
			DD-MEX	13.30	4.815×10^{-9}

In Tab. 2 we display the upper limit effective temperature (T_{∞}^{ul}) taken from [40, 41] of the four pulsars and the obtained radius (R_{NS}), distance from galactic center (d_{GC}) according to Appendix A, and the lower limit on v_{halo} (v_{halo}^{ll}) with the four different RMF models. We find that for any particular pulsar, the value of v_{halo}^{ll} does not differ very much for the different models. From Tab. 2, it is clear that for any given pulsar of a particular mass, the value of v_{halo}^{ll} is minimum for the model that gives the maximum radius. Our values of v_{halo}^{ll} are also consistent with i.e., less than the fitted values of v_{halo} obtained in [46] with respect to the d_{GC} of each pulsar.

3.2 Effective temperature from v_{halo} data

In Tab. 3 we tabulate the values of T_{∞} obtained for the four pulsars with the different models using the fitted values of v_{halo} with respect to d_{GC} from [46]. The obtained values of T_{∞} in Tab. 3 are consistent with i.e., less than the upper limit on T_{∞} prescribed in [40, 41]. It can be seen from Tab. 3 that for any particular pulsar, the value of T_{∞} differs negligibly for different models.

Table 3: Some known pulsars and their values of v_{halo} fitted from [46] and the obtained effective temperature (T_∞) with the four different RMF models.

Pulsar	v_{halo}	Model	$\log_{10} T_\infty$
J1906+0746	8.452×10^{-4}	TM1	3.989
		GM1	3.991
		DD2	3.993
		DD-MEX	3.985
J1933-6211	8.931×10^{-4}	TM1	3.928
		GM1	3.930
		DD2	3.932
		DD-MEX	3.925
J2043+1711	8.928×10^{-4}	TM1	3.927
		GM1	3.930
		DD2	3.931
		DD-MEX	3.924
Vela	8.994×10^{-4}	TM1	3.935
		GM1	3.935
		DD2	3.935
		DD-MEX	3.925

3.3 Dark matter scattering cross-section

In Fig. 1 we show the variation of threshold scattering cross-section of DM with the different particle species (viz., neutrons, protons, electrons and muons) with respect to mass of fermionic DM using the four models for the four individual pulsars. The results obtained with the four RMF models are displayed as bands in Figs. 1a, 1b, 1c and 1d for the pulsars J1906+0746, J1933-6211, J2043+1711 and the Vela pulsar, respectively. The value of threshold cross-section σ_{th}^i decreases initially when $q < k_i$ and then attains a constant value when $q = k_i$ (recalling Eq. 2.1). When $q < k_i$, the order of σ_{th}^i is almost same for J1906+0746, J1933-6211, and J2043+1711 ($\sim 10^{-39}$) and slightly higher than 10^{-40} in case of the Vela pulsar. We also find that the cross-section is minimum for neutrons while it is maximum for muons. This is because the muons populate the NS matter the least and hence N_μ is minimum compared to the other constituents while N_n is maximum. Therefore, from Eq. 2.1 it can be easily understood that σ_{th}^μ is maximum while σ_{th}^n minimum for all the pulsars. In Fig. 1 the bands signify the results from different RMF models. However, in case of Vela pulsar we obtain very negligible difference in the results of σ_{th}^n with the four models as seen from Fig. 1d. The values σ_{th}^n thus appear to be almost overlapping in Fig. 1d.

As discussed in Sec. 3.1, the capture rate is maximum. Hence the actual cross-section is always equal to the threshold cross-section i.e., $\bar{\sigma}_{\chi i} = \sigma_{th}^i$. In Fig. 2 we show the DM-electron scattering cross-section $\bar{\sigma}_{\chi e}$. Since the results of cross-section are almost same for the four different models, we choose to show the one obtained with DD2 model for the Vela pulsar in Fig. 2. We also compare the existing bounds from different direct detection experiments, taken from SENSEI [55], EDELWEISS [56], PandaX-II [57], XENON1T [58], SuperCDMS [59], DAMIC [60], and DarkSide-50 [10]. It is seen that our results are well beyond the explored region of the parameter space. Our estimates of $\bar{\sigma}_{\chi e}$ is also quite consistent with that obtained in [23].

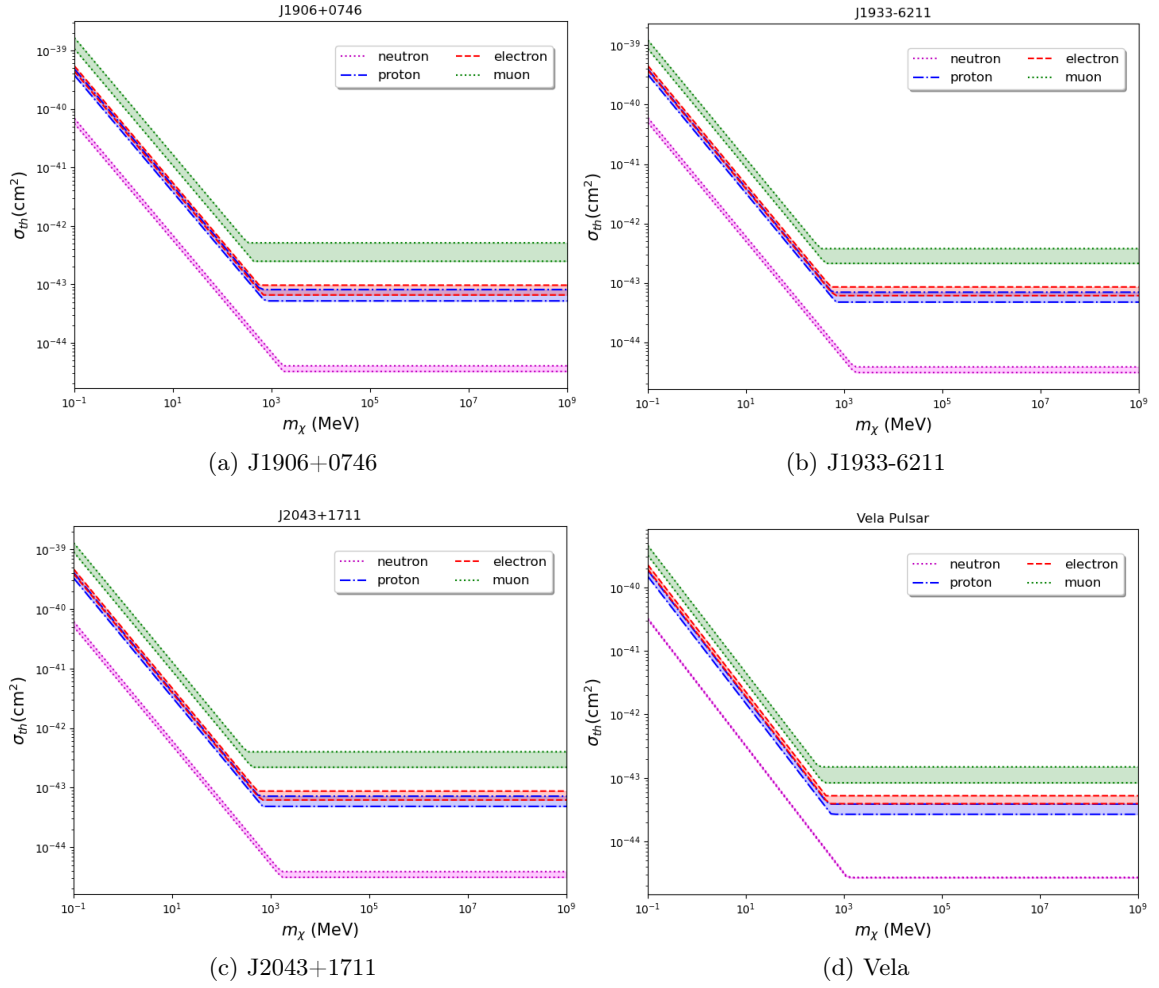


Figure 1: *Threshold scattering cross-section of dark matter with respect to mass of dark matter with neutrons, protons, electrons and muons obtained as range with the four models for the four pulsars.*

4 Summary and Conclusion

The present work revolves around the context of the kinetic heating of some known pulsars like J1906+0746, J1933-6211, J2043+1711 and the Vela pulsar due to the DM capture by them. For these pulsars, the mass, position with respect to the celestial sphere (RA and Dec) and distance from the earth are precisely measured to some extent. We utilize the EoS obtained with the well known RMF models (TM1, GM1, DD2 and DD-MEX) as the input to the TOV equations and obtain the radius of these four pulsars. The prediction of the radius and the radial profile of the number densities are a bit different for the different models considered. Therefore, for each pulsar, we obtain the threshold values of the interaction cross-section of DM with individual SM particles in NS to be of the same order for the different models. We compare the strongest scattering cross-section for the DM-electron interaction which is obtained for the Vela pulsar along with the experimentally explored region of the parameter space. Our prediction of the DM-electron scattering cross-section is a few order smaller than

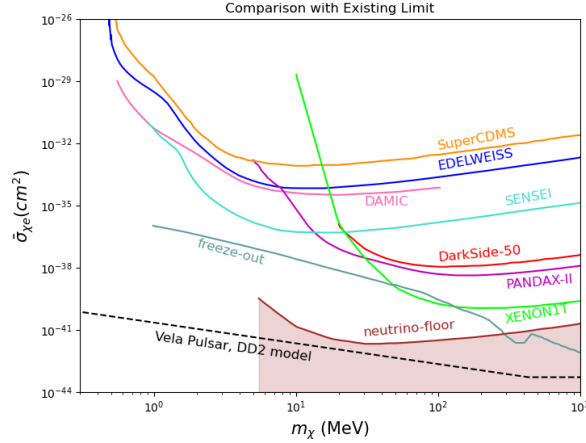


Figure 2: Actual scattering cross-section of dark matter with respect to mass of dark matter with electrons obtained with the DD2 model for the Vela pulsar. The existing bounds from different direct detection experiments are also compared which are taken from SENSEI [55], EDELWEISS [56], PandaX-II [57], XENON1T [58], SuperCDMS [59], DAMIC [60], and DarkSide-50 [10].

the values probed by the leading direct detection experiments and therefore this can act as a guide to the future developments of the direct and indirect searches of DM.

We extend our work to compute the lower bound on the halo velocity of DM from the knowledge of the upper bound on the effective temperature of the pulsars [40, 41]. This lower bound on v_{halo} is consistent with the results obtained from the analysis of the observational data [46].

On a different note we also estimate the value of T_∞ utilizing the observational findings of v_{halo} . Our estimates are consistent with the upper bound on T_∞ [40, 41].

Acknowledgements

Work of DS is supported by the NRF research Grants (No. 2018R1A5A1025563). Work of A.G. is supported by the National Research Foundation of Korea (NRF-2019R1C1C1005073).

A Distance of pulsars from galactic center

We obtain the distance d_{GC} of the four pulsars from galactic center using their individual RA and Dec and distance from earth ($d = r_2$). For the galactic center we also know that RA = 17h 45m 40.4s and Dec = 17° 00' 28.11" and the distance of the galactic center from the earth is $r_1 = 8.1$ kpc. Using the fact that $24\text{h} = 2\pi$, we can convert the RA's into radian as α and also using $1^\circ = \frac{\pi}{180}$, the Dec's can also be converted to radian as β .

Now in spherical polar coordinates, we have $\alpha = \phi$ and $\theta = \frac{\pi}{2} - \beta$. Thus the distance of any pulsar from galactic center is given as

$$d_{GC} = \sqrt{r_1^2 + r_2^2 - 2r_1r_2[\sin\theta_1\sin\theta_2\cos(\phi_1 - \phi_2) + \cos\theta_1\cos\theta_2]} \quad (\text{A.1})$$

where, (r_1, θ_1, ϕ_1) is the coordinate of the galactic center and (r_2, θ_2, ϕ_2) is that of a pulsar.

References

- [1] PLANCK collaboration, *Planck 2015 results. XIII. Cosmological parameters*, *Astron. Astrophys.* **594** (2016) A13 [[1502.01589](#)].
- [2] G. Bertone, D. Hooper and J. Silk, *Particle dark matter: Evidence, candidates and constraints*, *Phys. Rept.* **405** (2005) 279 [[hep-ph/0404175](#)].
- [3] PLANCK collaboration, *Planck 2018 results. VI. Cosmological parameters*, *Astron. Astrophys.* **641** (2020) A6 [[1807.06209](#)].
- [4] J.B. Bauer, D.J.E. Marsh, R. Hložek, H. Padmanabhan and A. Laguë, *Intensity Mapping as a Probe of Axion Dark Matter*, *Mon. Not. Roy. Astron. Soc.* **500** (2020) 3162 [[2003.09655](#)].
- [5] M. Lisanti, *Lectures on Dark Matter Physics*, in *Theoretical Advanced Study Institute in Elementary Particle Physics: New Frontiers in Fields and Strings*, pp. 399–446, 2017, DOI [[1603.03797](#)].
- [6] S. Profumo, *Astrophysical Probes of Dark Matter*, in *Theoretical Advanced Study Institute in Elementary Particle Physics: Searching for New Physics at Small and Large Scales*, pp. 143–189, 2013, DOI [[1301.0952](#)].
- [7] SUPERCDMS collaboration, *First Dark Matter Constraints from a SuperCDMS Single-Charge Sensitive Detector*, *Phys. Rev. Lett.* **121** (2018) 051301 [[1804.10697](#)].
- [8] XENON collaboration, *Search for New Physics in Electronic Recoil Data from XENONnT*, *Phys. Rev. Lett.* **129** (2022) 161805 [[2207.11330](#)].
- [9] PANDAX-II collaboration, *Results of dark matter search using the full PandaX-II exposure*, *Chin. Phys. C* **44** (2020) 125001 [[2007.15469](#)].
- [10] DARKSIDE collaboration, *Constraints on Sub-GeV Dark-Matter–Electron Scattering from the DarkSide-50 Experiment*, *Phys. Rev. Lett.* **121** (2018) 111303 [[1802.06998](#)].
- [11] SENSEI collaboration, *SENSEI: First Direct-Detection Constraints on sub-GeV Dark Matter from a Surface Run*, *Phys. Rev. Lett.* **121** (2018) 061803 [[1804.00088](#)].
- [12] LZ collaboration, *First Dark Matter Search Results from the LUX-ZEPLIN (LZ) Experiment*, *Phys. Rev. Lett.* **131** (2023) 041002 [[2207.03764](#)].
- [13] FERMI-LAT collaboration, *The Large Area Telescope on the Fermi Gamma-ray Space Telescope Mission*, *Astrophys. J.* **697** (2009) 1071 [[0902.1089](#)].
- [14] ICECUBE collaboration, *Observation of High-Energy Astrophysical Neutrinos in Three Years of IceCube Data*, *Phys. Rev. Lett.* **113** (2014) 101101 [[1405.5303](#)].
- [15] PAMELA collaboration, *An anomalous positron abundance in cosmic rays with energies 1.5–100 GeV*, *Nature* **458** (2009) 607 [[0810.4995](#)].
- [16] PAMELA collaboration, *Cosmic-Ray Positron Energy Spectrum Measured by PAMELA*, *Phys. Rev. Lett.* **111** (2013) 081102 [[1308.0133](#)].
- [17] AMS collaboration, *High Statistics Measurement of the Positron Fraction in Primary Cosmic Rays of 0.5–500 GeV with the Alpha Magnetic Spectrometer on the International Space Station*, *Phys. Rev. Lett.* **113** (2014) 121101.
- [18] M. Boudaud, J. Lavalle and P. Salati, *Novel cosmic-ray electron and positron constraints on MeV dark matter particles*, *Phys. Rev. Lett.* **119** (2017) 021103 [[1612.07698](#)].
- [19] CALET collaboration, *Energy Spectrum of Cosmic-Ray Electron and Positron from 10 GeV to 3 TeV Observed with the Calorimetric Electron Telescope on the International Space Station*, *Phys. Rev. Lett.* **119** (2017) 181101 [[1712.01711](#)].

- [20] O. Adriani et al., *Extended Measurement of the Cosmic-Ray Electron and Positron Spectrum from 11 GeV to 4.8 TeV with the Calorimetric Electron Telescope on the International Space Station*, *Phys. Rev. Lett.* **120** (2018) 261102 [[1806.09728](#)].
- [21] M. Baryakhtar, J. Bramante, S.W. Li, T. Linden and N. Raj, *Dark Kinetic Heating of Neutron Stars and An Infrared Window On WIMPs, SIMPs, and Pure Higgsinos*, *Phys. Rev. Lett.* **119** (2017) 131801 [[1704.01577](#)].
- [22] A. Joglekar, N. Raj, P. Tanedo and H.-B. Yu, *Relativistic capture of dark matter by electrons in neutron stars*, *Phys. Lett. B* **809** (2020) 135767 [[1911.13293](#)].
- [23] N.F. Bell, G. Busoni and S. Robles, *Capture of Leptophilic Dark Matter in Neutron Stars*, *JCAP* **06** (2019) 054 [[1904.09803](#)].
- [24] A. Joglekar, N. Raj, P. Tanedo and H.-B. Yu, *Dark kinetic heating of neutron stars from contact interactions with relativistic targets*, *Phys. Rev. D* **102** (2020) 123002 [[2004.09539](#)].
- [25] J. Bramante and N. Raj, *Dark matter in compact stars*, *Phys. Rept.* **1052** (2024) 1 [[2307.14435](#)].
- [26] W. Husain, T.F. Motta and A.W. Thomas, *Consequences of neutron decay inside neutron stars*, *JCAP* **10** (2022) 028 [[2203.02758](#)].
- [27] W. Husain and A.W. Thomas, *Novel neutron decay mode inside neutron stars*, *J. Phys. G* **50** (2023) 015202 [[2206.11262](#)].
- [28] W. Husain, D. Sengupta and A.W. Thomas, *Constraining Dark Boson Decay Using Neutron Stars*, *Universe* **9** (2023) 307 [[2306.07509](#)].
- [29] D. Zhou, *Neutron Star Constraints on Neutron Dark Decays*, *Universe* **9** (2023) 484.
- [30] A. Nelson, S. Reddy and D. Zhou, *Dark halos around neutron stars and gravitational waves*, *JCAP* **07** (2019) 012 [[1803.03266](#)].
- [31] D. Sen and A. Guha, *Implications of feebly interacting dark sector on neutron star properties and constraints from GW170817*, *Mon. Not. Roy. Astron. Soc.* **504** (2021) 3354 [[2104.06141](#)].
- [32] A. Guha and D. Sen, *Feeble DM-SM interaction via new scalar and vector mediators in rotating neutron stars*, *JCAP* **09** (2021) 027 [[2106.10353](#)].
- [33] A. Guha and D. Sen, *Constraining the mass of fermionic dark matter from its feeble interaction with hadronic matter via dark mediators in neutron stars*, *Phys. Rev. D* **Accepted** (2024) arXiv:2401.14419 [[2401.14419](#)].
- [34] S. Shakeri and D.R. Karkevandi, *Bosonic dark matter in light of the NICER precise mass-radius measurements*, *Phys. Rev. D* **109** (2024) 043029 [[2210.17308](#)].
- [35] D.R. Karkevandi, S. Shakeri, V. Sagun and O. Ivanytskyi, *Bosonic dark matter in neutron stars and its effect on gravitational wave signal*, *Phys. Rev. D* **105** (2022) 023001 [[2109.03801](#)].
- [36] C.H. Lenzi, M. Dutra, O. Lourenço, L.L. Lopes and D.P. Menezes, *Dark matter effects on hybrid star properties*, *Eur. Phys. J. C* **83** (2023) 266 [[2212.12615](#)].
- [37] O. Lourenço, C.H. Lenzi, T. Frederico and M. Dutra, *Dark matter effects on tidal deformabilities and moment of inertia in a hadronic model with short-range correlations*, *Phys. Rev. D* **106** (2022) 043010 [[2208.06067](#)].
- [38] N.F. Bell, G. Busoni, S. Robles and M. Virgato, *Improved Treatment of Dark Matter Capture in Neutron Stars II: Leptonic Targets*, *JCAP* **03** (2021) 086 [[2010.13257](#)].
- [39] H. Tananbaum, M.C. Weisskopf, W. Tucker, B. Wilkes and P. Edmonds, *Highlights and Discoveries from the Chandra X-ray Observatory*, *Rept. Prog. Phys.* **77** (2014) 066902 [[1405.7847](#)].

- [40] T. Prinz and W. Becker, *A Search for X-ray Counterparts of Radio Pulsars*, *Astrophys. J.* **resubmitted** (2015) arXiv:1511.07713 [1511.07713].
- [41] W. Becker, *A Search for X-ray Counterparts of Radio Pulsars*, in *AAS/High Energy Astrophysics Division #14*, vol. 14 of *AAS/High Energy Astrophysics Division*, p. 114.08, Aug., 2014.
- [42] Y. Sugahara and H. Toki, *Relativistic mean field theory for unstable nuclei with nonlinear sigma and omega terms*, *Nucl. Phys. A* **579** (1994) 557.
- [43] N.K. Glendenning and S.A. Moszkowski, *Reconciliation of neutron star masses and binding of the lambda in hypernuclei*, *Phys. Rev. Lett.* **67** (1991) 2414.
- [44] S. Typel, G. Ropke, T. Klahn, D. Blaschke and H.H. Wolter, *Composition and thermodynamics of nuclear matter with light clusters*, *Phys. Rev. C* **81** (2010) 015803 [0908.2344].
- [45] A. Taninah, S.E. Agbemava, A.V. Afanasjev and P. Ring, *Parametric correlations in energy density functionals*, *Phys. Lett. B* **800** (2020) 135065 [1910.13007].
- [46] P. Bhattacharjee, S. Chaudhury and S. Kundu, *Rotation Curve of the Milky Way out to ~ 200 kpc*, *Astrophys. J.* **785** (2014) 63 [1310.2659].
- [47] B.-N. Lu, E.-G. Zhao and S.-G. Zhou, *Quadrupole deformation (β, γ) of light Λ hypernuclei in constrained relativistic mean field model: shape evolution and shape polarization effect of Λ hyperon*, *Phys. Rev. C* **84** (2011) 014328 [1104.4638].
- [48] C.-J. Xia, T. Maruyama, A. Li, B.Y. Sun, W.-H. Long and Y.-X. Zhang, *Unified neutron star EOSs and neutron star structures in RMF models*, *Commun. Theor. Phys.* **74** (2022) 095303 [2208.12893].
- [49] R.C. Tolman, *Static solutions of Einstein's field equations for spheres of fluid*, *Phys. Rev.* **55** (1939) 364.
- [50] J.R. Oppenheimer and G.M. Volkoff, *On Massive neutron cores*, *Phys. Rev.* **55** (1939) 374.
- [51] H. Quaintrell, A.J. Norton, T.D.C. Ash, P. Roche, B. Willems, T.R. Bedding et al., *The mass of the neutron star in Vela X-1 and tidally induced non-radial oscillations in GP Vel*, *Astron. Astrophys.* **401** (2003) 313 [astro-ph/0301243].
- [52] D.G. Yakovlev and C.J. Pethick, *Neutron star cooling*, *Ann. Rev. Astron. Astrophys.* **42** (2004) 169 [astro-ph/0402143].
- [53] J.F. Navarro, C.S. Frenk and S.D.M. White, *The Structure of cold dark matter halos*, *Astrophys. J.* **462** (1996) 563 [astro-ph/9508025].
- [54] M. Bauer and T. Plehn, *Yet Another Introduction to Dark Matter: The Particle Physics Approach*, vol. 959 of *Lecture Notes in Physics*, Springer (2019), 10.1007/978-3-030-16234-4, [1705.01987].
- [55] SENSEI collaboration, *SENSEI: Direct-Detection Results on sub-GeV Dark Matter from a New Skipper-CCD*, *Phys. Rev. Lett.* **125** (2020) 171802 [2004.11378].
- [56] EDELWEISS collaboration, *First germanium-based constraints on sub-MeV Dark Matter with the EDELWEISS experiment*, *Phys. Rev. Lett.* **125** (2020) 141301 [2003.01046].
- [57] PANDAX-II collaboration, *Search for Light Dark Matter-Electron Scatterings in the PandaX-II Experiment*, *Phys. Rev. Lett.* **126** (2021) 211803 [2101.07479].
- [58] XENON collaboration, *Light Dark Matter Search with Ionization Signals in XENON1T*, *Phys. Rev. Lett.* **123** (2019) 251801 [1907.11485].
- [59] SUPERCDMS collaboration, *Constraints on low-mass, relic dark matter candidates from a surface-operated SuperCDMS single-charge sensitive detector*, *Phys. Rev. D* **102** (2020) 091101 [2005.14067].

- [60] DAMIC collaboration, *Constraints on Light Dark Matter Particles Interacting with Electrons from DAMIC at SNOLAB*, *Phys. Rev. Lett.* **123** (2019) 181802 [[1907.12628](#)].